Aerodynamic Hull Design for HASPA LTA Optimization

Fabio R. Goldschmied*
Westinghouse Electric Corporation, Pittsburgh, Pa.

The present design estimates for the Navy concept of a high-altitude superpressure powered aerostat (HASPA) are 800,000 ft^3 hull volume at an altitude of 70,000 ft, with a maximum required speed of 30 knots. Both the hull weight and the propulsion power must be minimized for a successful vehicle design. On the basis of extensive wind-tunnel tests at the HASPA volume Reynolds number ($R_v = 2.16 \times 10^6$), a 3:1 body has been selected for minimum hull weight, and its propulsion power requirements are 1.80 kW, including appendage drag and stern wake propeller efficiency. Passive boundary-layer control is applied to the aftbody by means of a Ringleb cusp at 82% length. On the forebody, the boundary layer remains laminar up to 77% length, as shown by China Clay wind-tunnel flow visualization at the exact HASPA Reynolds number.

Nomenclature

a = ambient sound velocity, fps
C_D = drag coefficient based on volume
C_p = static pressure coefficient
C_{HP} = power coefficient based on volume
D = maximum hull diameter, ft
g = BLC slot width, ft
L = hull length, ft
R_L = Reynolds number based on length
R_v = Reynolds number based on volume
T_o = ambient temperature, °F
U_o = flight velocity, fps
V = hull volume, ft^3
x = hull axial distance, ft
X_t = axial transition location, ft
γ = air density, lb/ft^3
ν = kinematic viscosity, ft^2/s

Introduction

THE development of high-altitude unmanned powered aerostats has attracted considerable Navy interest in recent years. A discussion of the studies underlying the high-altitude superpressure powered aerostat (HASPA) program is well-presented by Wessel and Petrone.[1] A history of other earlier high-altitude aerostat projects is given by Korn.[2]

An altitude of 70,000 ft was selected from the beginning, because it is the so-called "crossover altitude" where winds are generally very light and averaging 10 knots (below 30 knots) and variable in direction. At that altitude, the line-of-sight coverage comprises some 400,000 sq. miles or a radius of 350 miles. The HASPA system will be launched like a high-altitude balloon, will operate like a nonrigid airship (unmanned), and will have mission capabilities comparable to a low-altitude stationary satellite. Potential nonmilitary uses of the vehicle include communications relay, environmental monitoring, and ship traffic control.

A detailed stationkeeping analysis of the HASPA vehicle has been carried out by Hill et al.[3]; it is seen that the useful on-station time increases with the maximum aerostat velocity available and a velocity of 30 knots is recommended.

The latest description of the HASPA airship is given by Pretty and Hookway[4] as 800,000 ft^3, 5:1 fineness ratio with a stern wake propeller, and four triangular tail fins (1200 ft^2 each). The length is given as 333 ft and the diameter as 66.7 ft.

Received Jan. 12, 1978; revision received April 28, 1978.

Index category: Lighter-than-Airships.

*Advisory Scientist, Research and Development Center. Associate Fellow AIAA.

In the earlier paper by Wessel and Petrone,[1] the HASPA volume was stated to be $\approx$1,000,000 ft^3 with a volumetric drag coefficient of $C_D = 0.05$ and a propulsive efficiency of 75%. At 30 knots, the propulsive power would then be 10 hp. Since the static lift of helium at 70,000 ft is 0.004 lb/ft^3, the total gross weight of the 800,000 ft^3 vehicle will be only 3200 lb; thus, it is abundantly clear that hull weight and power must be reduced to the absolute minimum.

Aerodynamic Analysis

The HASPA aerodynamic parameters are as follows:

Hull volume: $V = 800{,}000$ ft^3
Flight speed (30 knots): $U_o = 50$ fps
Air density at 70,000 ft: $\gamma = 0.00448$ lb/ft^3
Kinematic viscosity at 70,000 ft: $\nu = 0.002143$ ft^2/s
Temperature at 70,000 ft: $T_o = -67$°F
Speed of sound at 70,000 ft: $a = 970$ fps
Volume Reynolds number: $R_v = U_o V^{1/3}/\nu = 2.16 \times 10^6$

The problem is to determine the hull design which would minimize both hull weight and propulsion power at the volume Reynolds number of $R_v \cong 2 \times 10^6$.

As regards the relative hull weights, Ref. 5 (Appendix D) indicates that a 5:1 hull (as proposed in Ref. 4) would weigh ~50% more than a 3:1 hull for nonrigid pressurized airships of any size, as shown in Table 1. Thus, a 3:1 hull would save at least 500 lb, which would be used for payload or fuel or reduction of hull volume. The aerodynamic problem has now been defined in terms of fineness-ratio (3.0) and flight Reynolds number ($R_v = 2.16 \times 10^6$).

First, a "reference" drag will be determined from test data of conventional streamline bodies in the wind tunnel and towing tank with free transition. Since the exact Reynolds number is achieved in the wind-tunnel and towing tank, it would be wrong to trigger transition artificially on the test model by wire trips, roughness strips, etc.

The following bodies are considered: 1) "Akron" model 5.9:1 – Ref. 6; 2) metalclad airship model 4.5:1 – Ref. 6; and 3) Navy series 58, fineness ratios from 4.0 to 10.0 – Ref. 7.

Table 1 Typical relative hull weight fractions

Fineness ratio	LTA speed, knots 60	90	120	150
3.0	1.000	1.224	1.410	1.581
4.5	1.379	1.689	1.953	2.170
6.0	1.744	2.139	2.465	2.759

Table 2 Summary of hull drag

Model	$R_v = 2.16 \times 10^6$ L/D	R_L ($\times 10^6$)	Free transition C_D	Test
"Akron"	5.9	8.64	0.0240	W-T[a]
Metalclad	4.5	7.51	0.0240	W-T
4154	4	6.81	0.0212	T-T[b]
4176	5	8.36	0.0218	T-T
4168	7	9.89	0.0232	T-T
4160	7	9.89	0.0233	T-T
4175	5	8.11	0.0233	T-T
4163	7	9.89	0.0241	T-T
4156	6	8.92	0.0243	T-T
4177	7	9.89	0.0248	T-T
4155	5	7.88	0.0249	T-T
4164	7	10.45	0.0252	T-T
4165	7	10.16	0.0252	T-T
4174	7	9.89	0.0252	T-T
4171	7	9.89	0.0254	T-T
4170	7	9.89	0.0255	T-T
4166	7	9.65	0.0257	T-T
4161	7	9.89	0.0262	T-T
4158	8	10.80	0.0265	T-T
4159	10	12.54	0.0274	T-T

[a] Wind-tunnel air tests (Ref. 6).
[b] Towing-tank water tests (Ref. 7).

Table 3 Summary of "Dolphin" water-drop tests

$R_v(\times 10^6)$	C_D	$R_v(\times 10^6)$	C_D
5.62	0.0138	10.2	0.0079
5.58	0.0092	11.0	0.0080
7.33	0.0081	11.0	0.0086
7.50	0.0110	11.55	0.0104
8.43	0.0087	12.90	0.0084
8.70	0.0065	13.25	0.0103
9.25	0.0079	13.70	0.0090
9.27	0.0093	14.15	0.0089

Table 4 Summary of DTMB wind-tunnel test data (Ref. 8), zero slot suction, triggered transition

L/D	Slot, g/L	C_D	$R_L(\times 10^6)$	$R_v(\times 10^6)$
4.20	–	0.0262	8.57	2.63
3.00	0.00	0.0438	7.00	2.64
3.00	0.016	0.0308	6.95	2.62
3.00	0.008	0.0274	7.20	2.71
3.00	0.008	0.0291	6.85	2.58
3.00	0.004	0.0286	6.90	2.60

1) A metal model 37.39 in. long was used, without any boundary-layer trip. For $R_v = 2.16 \times 10^6$, the length Reynolds number was $R_L = 8.64 \times 10^6$ and the drag coefficient was $C_D = 0.024$. The wind-tunnel was the old variable-density facility at the NASA Langley Research Center.

2) A polished metal model 45.55 in. long was used, without any boundary-layer trip. For $R_v = 2.16 \times 10^6$, the length Reynolds number was $R_L = 7.51 \times 10^6$ and the drag coefficient was $C_D = 0.024$. Fins and cars were also added to the model; the fins drag increment was $\Delta C_D = 0.003$ and the increment for both fins and cars was $\Delta C_D = 0.004$. The wind tunnel was the old variable-density facility at the NASA Langley Research Center.

3) Mahogany models 108 in. long were used without any boundary-layer trip. For $R_v = 2.16 \times 10^6$, the length Reynolds number would change with fineness ratio and shape, as tabulated later. The tests were carried out in water in the towing tank of the David W. Taylor Model Basin.

The summary of all drag data is shown in Table 2 for a constant value of $R_v = 2.16 \times 10^6$ and free-transition testing.

It can be seen that at this Reynolds number, bodies with fineness ratios of 4.0 are as good or better than bodies with ratios of 5 or 5.9. In any event, the drag range between the best and the worst body is not large, i.e., of the order of 30%. For a given propulsion power, this means a 10% speed change.

Thus, in conclusion, $C_D = 0.0212$ may be the "reference" drag against which all 3:1 results will be assessed. Similarly, the 4.0:1 fineness ratio may be the "reference" value for hull weight evaluation, with an estimated relative hull weight fraction of 1.25, or 25% higher than that of the 3:1 hull.

The next level of aerodynamic sophistication is that provided by Carmichael[14] with the development and water-drop test of the "Dolphin" of 3.3:1 fineness ratio with free transition. The only aftbody boundary-layer control was that provided by shape alone. Laminar flow extended to ~55% length up to a Reynolds number $R_v \sim 14 \times 10^6$. The tail assembly was mounted on an extended tailboom, rather than on the aftbody itself, to avoid triggering aftbody flow separation and to gain leverage. For the record, a summary of Carmichael's drag results is given in Table 3. Extrapolating back to $R_v \sim 2.16 \times 10^6$ from the tabulated value of $C_D = 0.0138$ at the lowest $R_v = 5.62 \times 10^6$, a value of $C_D \sim 0.018$ is the highest that can be expected.

The final aerodynamic problem is now focused on the design of a 3:1 body with passive aftbody BLC, which would achieve a drag coefficient $C_D \leqq 0.0212$ at $R_v = 2.16 \times 10^6$. It is to be remembered that the metalclad ZMC-2,2.95:1 airship had a flight power coefficient $C_{HP} = 0.055$ at $R_L = 10^8$, including fins and propulsive efficiency. Assuming the latter to have been 75% and the drag increment to have been $\Delta C_D = 0.005$, the bare hull drag coefficient is estimated to be $C_D = 0.036$. Extrapolating the drag back to $R_L \approx 6 \times 10^6$, it is estimated that $C_D \approx 0.045$ (triggered transition) or 0.040 (free transition). Another body of similar fineness ratio (3:1) was tested by Cerreta[8] in the wind tunnel with triggered transition at $R_v = 2.64 \times 10^6$, yielding a drag coefficient of $C_D = 0.0438$ for the basic body; this is in good agreement with the ZMC-2 extrapolation. Unfortunately, Cerreta did not carry out free-transition tests.

The main purpose of the Cerreta[8] test program was to investigate the aerodynamic airship design proposed by Goldschmied[9] with application of aftbody boundary-layer control by single-slot suction. It has not been widely recognized, however, that he achieved, as an unplanned result, passive boundary-layer control by means of a Ringleb cusp effect in the suction slot entrance for the case of zero suction flow. Indeed, a drag coefficient of $C_D = 0.0274$ was achieved at $R_v = 2.71 \times 10^6$, to be compared with $C_D = 0.0438$ at the same Reynolds number for the basic 3:1 body with the slot closed; the drag reduction is 37%.

In Table 4, a drag summary of the Cerreta results for zero slot suction, including a test of the 4.2:1 XZS2G-1 blimp model as reference, is presented.

Comparing the drag coefficients of Table 2 (free transition) with those of Table 4 (triggered transition), it is quite surprising to note that $C_D = 0.0274$ is not that much larger than the best $C_D = 0.0212$ for conventional streamlined bodies.

The Cerreta test model was resurrected in 1969 for a new wind-tunnel test program by the Westinghouse Electric Corporation with many new slot configurations and improved instrumentation. A set of tests was carried out with free transition to investigate the matter of passive aftbody boundary-layer control. The best configuration yielded a drag coefficient of $C_D = 0.0144$ at the volume Reynolds number of $R_v = 3.13 \times 10^6$; laminar boundary-layer flow was maintained up to ~70% body length by actual wind-tunnel China Clay visualization. The Westinghouse test results for free transition are summarized in Table 5. A summary may be presented for

Table 5 Summary of Westinghouse wind-tunnel data

L/D	Slot, g/L	C_D	$R_L(\times 10^6)$	$R_v(\times 10^6)$
3.0	0.0009	0.0154	8.3	3.13
3.0	0.004	0.0144	8.3	3.13
3.0	0.0069	0.0231	8.3	3.13
3.0	0.0120	0.0242	8.3	3.13
3.0	0.0154	0.0241	8.3	3.13

the aerodynamic options available with free transition at a common volume Reynolds number $R_v \sim 3.1 \times 10^6$ (to allow ample margin above 2.16×10^6):

1) Best conventional streamlined 4:1 body: $R_L = 10 \times 10^6$, $C_D = 0.0235$, and the relative hull weight fraction is 1.25.

2) Carmichael 3.3:1 "Dolphin": $R_L = 9.1 \times 10^6$, $C_D \cong 0.017$, and the relative hull weight fraction is 1.15.

3) Goldschmied 3:1 body with cusp: $R_L = 8.3 \times 10^6$, $C_D = 0.0144$, and the relative hull weight fraction is 1.00.

The propulsive efficiency of a stern wake propeller for an axisymmetric streamlined body has been investigated in the wind tunnel by McLemore[9] and found experimentally to be 103% (on the basis of flight velocity). A stern propeller would induce an accelerated flowfield over the aftbody and thus would be beneficial, since the boundary-layer growth would be decreased and turbulent separation delayed. In any event, a complete wind-tunnel test of the body with stern propeller should be carried out to optimize the mutual interaction.

In conclusion, the following aerodynamic characteristics may be accepted for the HASPA vehicle:

Volume Reynolds number: $R_v = 2.16 \times 10^6$
Hull (3:1) drag coefficient: $C_D = 0.0150$
Empennage drag increment: $\Delta C_D = 0.003$
Total vehicle drag coefficient: $C_D = 0.018$
Propulsive efficiency: 103%

Optimum Hull Design

The selected 3:1 aerodynamic hull design will be presented in detail, including the boundary-layer control cusp. The basic body profile was proposed by Goldschmied[10] and is given in tabular form (44 coordinate points) by Cerreta (Ref. 8, p. 16) and by Goldschmied (Ref. 11, Table 1). The inviscid pressure distribution of the best experimental configuration is given in Fig. 1 for three angles of attack (0, 6, and −6 deg). The body at 0 deg is designed to have a negative pressure gradient (decreasing pressure) over the forebody which extends up to 82% length; then a steep pressure rise is achieved over a very short axial distance, corresponding almost to a step change, followed by a very short aftbody with negative pressure gradient. No significant pressure gradient changes are caused by the ±6 deg angle-of-attack range in terms of boundary-layer behavior. The 82% length forebody is intended to maximize the extent of laminar boundary layer with consequent low skin friction; in fact, transition was observed by

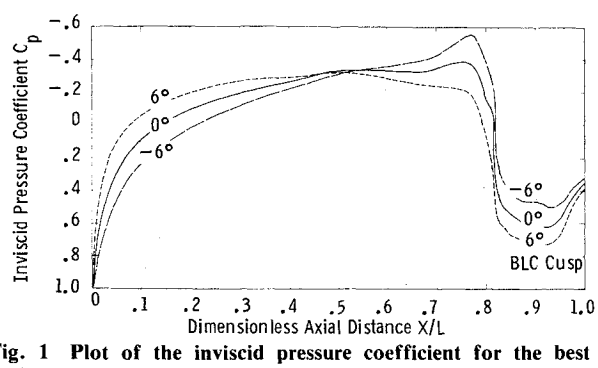

Fig. 1 Plot of the inviscid pressure coefficient for the best experimental configuration for angles of attack of 0, −6, and +6 deg.

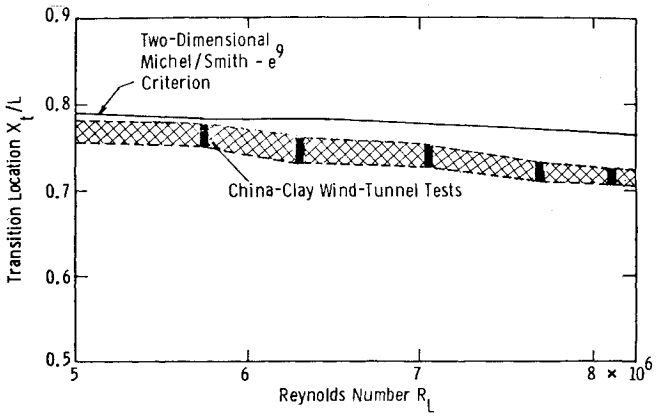

Fig. 2 Experimental verification of Michel/Smith transition criterion against wind-tunnel test data.

China Clay[16] flow visualization in the wind tunnel as far back as 77%. Figure 2 presents the trend of transition location against Reynolds number; it is seen that the two-dimensional Michael/Smith e^9 criterion is well-verified throughout the test range. Axisymmetric transition prediction, however, departs from the two-dimensional method at some Reynolds number, which is a complex function of body shape. An iterative transition prediction algorithm for axisymmetric bodies is given by Goldschmied.[12,13]

Figure 3 presents four China Clay[16] flow visualization photos of the present test model in the wind tunnel. The top left and bottom right photos show normal transition; the white area indicates turbulent flow while the dark area indicates laminar flow. The top right photo represents transition triggered artifically at 10% length; the body is all uniformly white after the nose. The bottom left photo shows two classical turbulence 13 deg wakes, as originated by some roughness spots; the wakes are white while the rest of the forebody is dark. Since the 8.5 × 12 ft wind tunnel† was not a low-turbulence facility and the China Clay technique produced a rather rough surface finish, a high-degree of confidence may be placed on these laminar flow results. It is also noticeable that transition occurred downstream of a mechanical joint in the model structure. In conclusion, for this aerodynamic hull design at the HASPA Reynolds number ($R_L = 5.75 \times 10^6$), laminar flow will extend to a record-breaking 77% length, with an observed 50% safety margin in terms of higher Reynolds number.

Some sort of boundary-layer control, active or passive, must be installed at 82% length to help the boundary layer to overcome the steep adverse pressure gradient and to prevent massive flow separation. Active BLC is based on a single suction slot at 82% length, whereby 25-45% of the local boundary-layer mass flow is ingested, restored to freestream total-head by an axial blower, and ejected at the stern. This type of system is well-discussed by Goldschmied.[11] For HASPA application, however, passive BLC is simpler and adequate for the first generation of vehicles. The classical device for passive BLC is the Ringleb[15] cusp. A workable cusp effect is achieved by the suction slot entrance configuration in the absence of suction. Figures 4 and 5 show the aftbody configurations that proved successful in achieving low drag ($C_D \sim 0.015$) without any slot suction; it is seen that the aftbody is well inside the "ideal" profile. The static pressure distribution on the complete test body with the cusp of Fig. 5 is shown in Fig. 6 for two cases: 1) angle of attack $\alpha \sim 0$ deg, free transition (experimental); and 2) angle of attack $\alpha \sim -6$ deg, free transition (experimental). It is seen that the cusp passive BLC cannot achieve the stepwise

†McDonnell 8.5 × 12 ft low-speed wind tunnel, 230 mph, turbulence factor (3.00 in. diam. sphere) of 1.16, St. Louis, Mo.

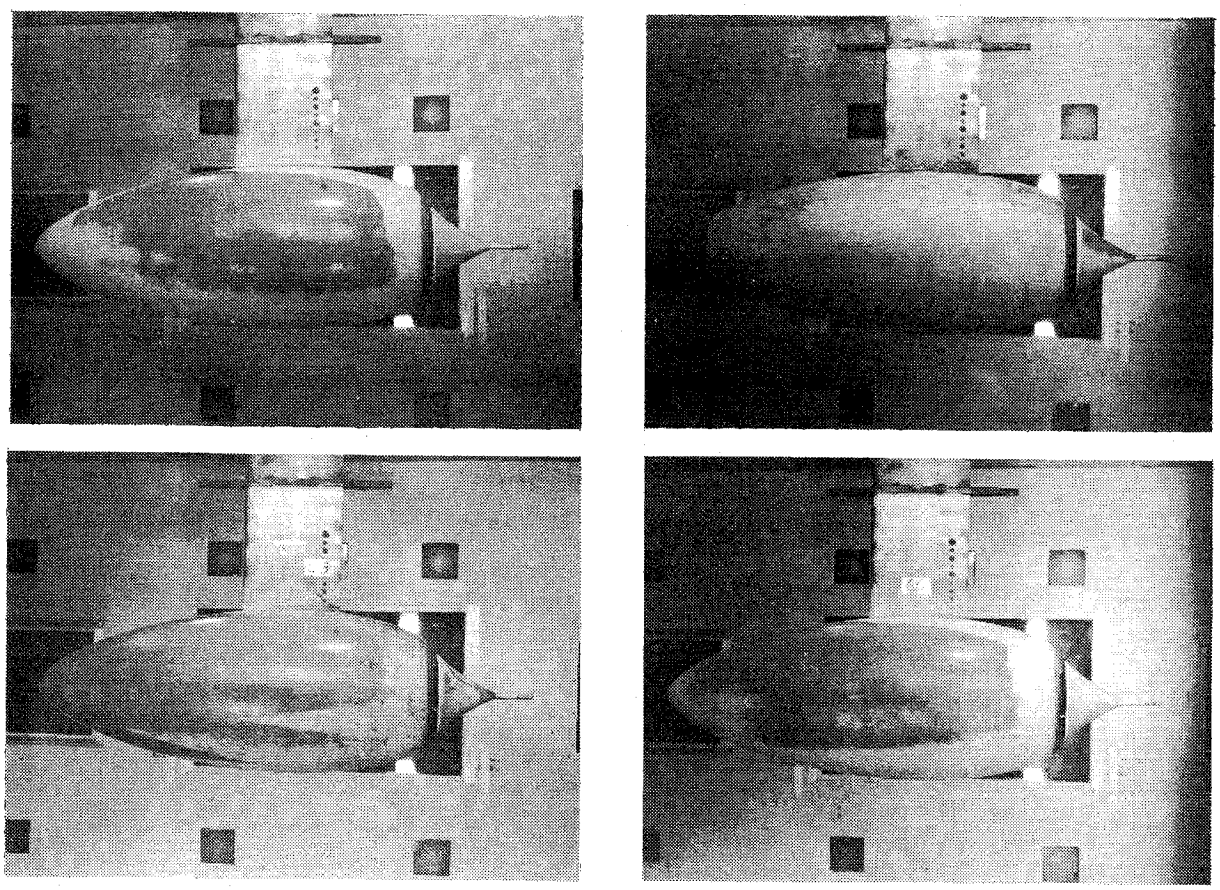

Fig. 3 Transition visualization by China-Clay technique in wind tunnel.

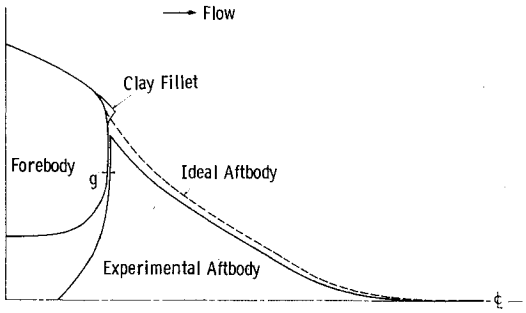

Fig. 4 First test configuration for cusp BLC, $g = 0.0625$ in.

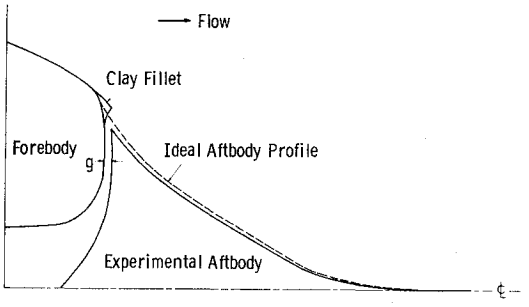

Fig. 5 Second test configuration for cusp BLC, $g = 0.235$ in.

pressure gradient of the inviscid pressure distribution of Fig. 1, but it does achieve in the wind tunnel the correct final pressure at the trailing point of the body ($C_p = 0.4$).

Figure 7 presents the static-pressure coefficient plot for separated aftbody flow for two cases: 1) angle of attack $\alpha \sim 0$ deg, tripped transition (experimental); and 2) angle of attack $\alpha \sim -6$ deg, tripped transition (experimental). In these cases,

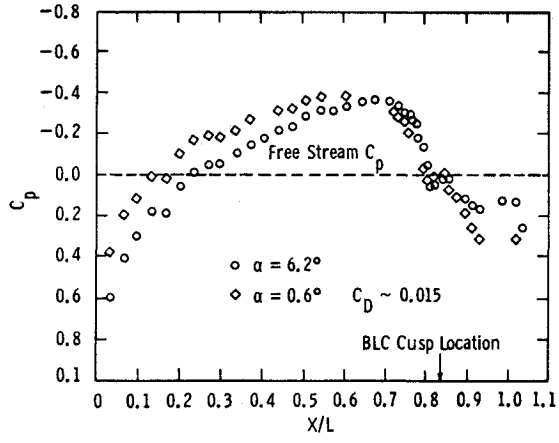

Fig. 6 Static-pressure coefficient distribution with cusp vortex effect and free transition.

the aftbody pressure recovery is much less, reaching only $C_p = 0.1$.

Figure 8 shows the HASPA aftbody with the cusp configuration.

The dimensions of the 3:1 hull for 800,000 ft^3 volume will be 246 ft length and 82 ft maximum diameter. Laminar boundary layer will extend to 189 ft from the nose. Including empennage drag and propulsive efficiency, the propulsion power will be 2.38 hp or 1.80 kW at 70,000 ft altitude. If transition should move upstream from 189 ft to 25 ft from the nose, then the power will go up to 3.65 hp or 2.75 kW; this is the worst possible case for this hull design.

For propulsion and control, it is expected to employ a pivoted motor/propeller unit; this should be practical in view of the large hull size and very low power (~2.5 hp). For the

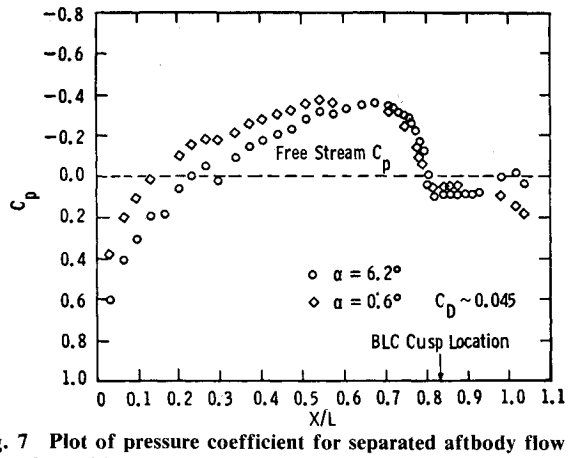

Fig. 7 Plot of pressure coefficient for separated aftbody flow with tripped transition.

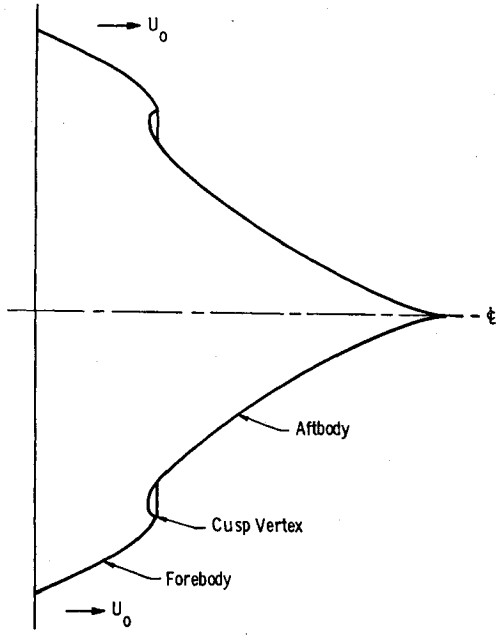

Fig. 8 Typical cusp BLC aftbody design.

empennage, it is visualized to employ an annular "ring" airfoil of pressurized fabric construction installed by a suitable tension-wire harness. The structural and weight constraints would interact strongly with the aerodynamics in the tail/aftbody optimization; considerable wind-tunnel test work remains to be done.

Conclusions

Several significant conclusions have emerged from this brief study:

1) At the HASPA volume Reynolds number of $R_v = 2.16 \times 10^6$, the best conventional streamlined body with free transition has a fineness ratio of 4:1, a drag coefficient of $C_D = 0.0212$, and a relative hull weight fraction of 1.25.

2) A 3:1 body with aftbody cusp BLC at 82% length has a drag coefficient of $C_D = 0.015$ with free transition and of $C_D = 0.0272$ with transition triggered at 10% length. Thus, it is entirely practical to have *both* minimum hull weight and minimum propulsion power. The relative hull weight fraction is 1.00.

3) With the 3:1 body, laminar flow can be reliably had up to ~70% length, with ample aerodynamic margin at $R_v = 2.16 \times 10^6$.

4) The HASPA 800,000 ft^3 3:1 hull will be 246 ft long with a maximum diameter of 82 ft. The propulsion power will be 1.80 kW, including empennage drag and propulsive efficiency.

5) Wind-tunnel tests are needed to establish the best power performance of the body with stern propeller and ring tail before actual vehicle design can begin.

Acknowledgment

This study was funded by the Westinghouse corporate research program.

References

[1] Wessel, P.R. and Petrone, F.J., "Special Problems and Capabilities of High Altitude Lighter-Than-Air Vehicles," *Proceedings of the Interagency Workshop on Lighter-Than-Air Vehicles,* NASA CR-137800, Jan. 1975, pp. 595-603.

[2] Korn, A.O., "Unmanned Powered Balloons," *Proceedings of the Interagency Workshop on Lighter-Than-Air Vehicles,"* NASA CR-137800, Jan. 1975, pp. 585-594.

[3] Hill, M.L., Pasierb, J.J., Weiss, R.O., and Whyte, T.R., "Station-Keeping Analysis of the HASPA Vehicle in the Northern Hemisphere," AIAA Paper 77-1191, Melbourne, Fla., Aug. 1977.

[4] Pretty, J.R., and Hookway, R.D., "A Comparison of Different Forms of Dirigible Equations of Motion," AIAA Paper 77-1179, Melbourne, Fla., Aug. 1977.

[5] Lancaster, J.W., "Feasibility Study of Modern Airships. Phase I: Volume IV-Appendices," NASA CR-137692, Aug. 1975.

[6] Abbott, H., "The Drag of Two Streamline Bodies as Affected by Protuberances and Appendages," NACA Rept. 451, 1932.

[7] Gertler, M., "Resistance Experiments on a Systematic Series of Streamlined Bodies of Revolution – for Application to the Design of High-Speed Submarines," U.S. Navy TMB Rept. C-297, Apr. 1950.

[8] Cerreta, P.A., "Wind-Tunnel Investigation of the Drag of a Proposed Boundary-Layer-Controlled Airship," U.S. Navy TMB Aero Rept. 914, March 1957.

[9] McLemore, H.C., "Wind-Tunnel Tests of a 1/20 Scale Airship Model with Stern Propellers," NASA TN D-1026, Jan. 1962.

[10] Goldschmied, F.R., "Proposal for the Study of Application of Boundary-Layer Control to Lighter-Than-Air Craft," Goodyear Aircraft Corporation, GER5796, Jan. 1954.

[11] Goldschmied, F.R., "Integrated Hull Design, Boundary-Layer Control and Propulsion of Submerged Bodies," *AIAA Journal of Hydronautics,* Vol. 1, July 1967, pp. 2-11.

[12] Goldschmied, F.R., "Axisymmetric Transition: Correlation of the Maximum Reynolds Number Limiting Applicability of the Two-Dimensional Michel/Smith Criterion to an Arbitrary Body," Low-Speed Boundary-Layer Transition Workshop, RAND Corporation, Santa Monica, Calif., Rept. R-1752-ARPA/ONR, June 1975.

[13] Goldschmied, F.R., "Transition Prediction Algorithm for Axisymmetric Submerged Bodies," U.S. Navy Sea Systems Command Hydromechanics Committee – 1974 Annual Meeting, Newport, R.I., Oct. 1974.

[14] Carmichael, B.H., "Underwater Drag Reduction Through Choice of Shape," AIAA Paper 66-657, Colorado Springs, Co., July 1966.

[15] Ringleb, F.O., "Separation Control by Trapped Vortices," *Boundary-Layer and Flow Control,* edited by G.V. Lachmann, Vol. 1, Pergamon Press, New York, 1961.

[16] Richards, E.J. and Burstall, F.H., "The China Clay Method of Indicating Transition," British ARC R&M 2126, Aug. 1945.